Research Square

Preprints are preliminary reports that have not undergone peer review.
They should not be considered conclusive, used to inform clinical practice,
or referenced by the media as validated information.

Modelling the potential impact of ash dieback disease on emerald ash borer spread in Great Britain

Matt Combes

combesmatt87@gmail.com

University of Warwick School of Life Sciences https://orcid.org/0009-0004-1889-3430

Vasthi Alonso Chávez

Rothamsted Research

Alice Milne

Rothamsted Research

Nathan Brown

Forest Research

Stephen Parnell

University of Warwick School of Life Sciences

Research Article

Keywords: Agrilus planipennis, Hymenoscyphus fraxineus, Fraxinus, biological invasion, tree mortality, tree health

Posted Date: November 19th, 2026

DOI: https://doi.org/10.21203/rs.3.rs-11542774/v1

License: This work is licensed under a Creative Commons Attribution 4.0 International License.
Read Full License

Modelling the potential impact of ash dieback disease on emerald ash borer spread in Great Britain

Matt Combes[1,2*], Vasthi Alonso Chávez[3], Alice Milne[3], Nathan Brown[4], Stephen Parnell[1,2]

[1] Warwick Crop Centre, University of Warwick, Stratford-upon-Avon, UK

[2] Zeeman Institute for Systems Biology and Infectious Disease Epidemiology Research, University of Warwick, Coventry, UK

[3] Rothamsted Research, Harpenden, UK

[4] Forest Research, Farnham, UK

* Corresponding author

E-mail: combesmatt87@gmail.com

ORCID:

Matt Combes 0009-0004-1889-3430; Vasthi Alonso Chávez 0000-0003-3506-7603; Alice Milne 0000-0002-4509-0578; Nathan Brown 0000-0003-3590-0538; Stephen Parnell 0000-0002-2625-4557

Acknowledgements

We thank the United Kingdom's Research and Innovation (UKRI) Programme for funding the work through through the Natural Environment Research Council (NERC) (https://www.ukri.org/councils/nerc/) (Project: NE/T007729/1).

Abstract

The epidemiology of tree pests and diseases is typically considered in isolation, but this is becoming increasingly unrealistic in the context of their co-occurrence. In Europe, the emerald ash borer (EAB) is spreading through an ash (*Fraxinus* spp.) population already afflicted by ash dieback disease (ADB). Both cause considerable ash mortality, but the impacts of ADB on EAB spread at the landscape scale have not been considered. Using Great Britain (GB) as a case study, we first develop a compartmental model to estimate distributions of ADB severity using data from the European literature. Next, we combine these ADB severity distributions for GB with a population dynamics model for EAB to explore ADB impacts on EAB spread. Our results provide the first landscape scale spatial estimates demonstrating variable ADB impact in GB and show that ADB will likely slow EAB spread mainly via removal of available hosts, with impacts depending on host availability in both the arrival location and wider landscape. Greater attraction of EAB to ADB stressed trees also slows EAB spread via elevated density-dependent larval mortality. We find that delaying EAB arrival and a higher ADB progress rate can further slow EAB spread, whilst greater survival of EAB larvae on ADB affected trees can greatly increase EAB spread. We highlight critical knowledge gaps and provide essential insights to inform effective EAB surveillance and control strategies. Our findings demonstrate the need for spatial datasets on current tree pest and disease impacts to facilitate better preparedness for emerging tree health threats.

Keywords: *Agrilus planipennis*; *Hymenoscyphus fraxineus*; *Fraxinus*; biological invasion; tree mortality; tree health

Introduction

Tree pests and diseases have been occurring at an increasing frequency since the Industrial Revolution. This is exemplified by an exponential increase of invasive forest pathogens in Europe (Santini et al. 2013), whilst non-native insect introductions to US forests have been occurring at a rate of ~2.5 per year (Lovett et al. 2016) (from hereon in plant pests and pathogens are collectively referred to as pests in line with international standards (IPPC Secretariat 2025)). This has consequences for both agricultural and commercial forestry systems, as well as natural and semi-natural systems. For example, *Phytophthora ramorum* is an oomycete of Asian origin (Jung et al. 2021) that is now estimated to result in annual direct damage costs of up to > €100 million yr^{-1} to both larch and beech in Europe (Kartakis et al. 2026), whilst also causing deaths of millions of oak and tanoak in the United States (Cobb et al. 2020). *Xylella fastidiosa*, a bacteria likely introduced to Europe via an imported coffee plant (Sicard et al. 2021) threatens not only EU olive production (Schneider et al. 2020), but also a wide range of European forest species (Desprez-Loustau et al. 2021).

Recent meta-analyses examining the potential impacts of tree pests and diseases in Britain, and tree pests in Europe state the need for future research to address both the additive and interactive effects among co-occurring pests (Bebber et al. 2025; Hlásny et al. 2025). However most epidemiological studies continue to consider individual pest species in isolation. In particular, to our knowledge, there is yet to be an epidemiological study on the impacts of an endemic tree disease on the invasion of a new insect pest. Furthermore, despite efforts to map distributions of pests, their impacts are not currently considered in the context of understanding how this may affect future pest outbreaks.

This is particularly pertinent given the multiple threats that ash species (*Fraxinus*) now face. *Fraxinus excelsior* and *Fraxinus angustifolia* have been heavily impacted by ash dieback disease (ADB) (George et al. 2022). This is a fungal disease caused by the invasive ascomycete *Hymenoscyphus fraxineus* (Kowalski 2006). The fungus is native to East Asia, where it colonises Asian ash species, causing no noticeable dieback (Cleary et al. 2016) but on European (*F. excelsior*) and narrow leaved ash (*F. angustifolia*), the disease can be devastating. Only a small fraction of trees are genetically resistant to the disease (McKinney et al. 2014), and it is estimated that at the landscape scale, approximately 50% of ash trees may die within 30 years after disease arrival (George et al. 2022), although this will be influenced by both stand and environmental factors (Combes et al. 2024).

Meanwhile, emerald ash borer beetle (EAB), which is also native to East Asia and associated with Asian ash (*Fraxinus mandshurica*) (Wei et al. 2004), was detected in North America in 2002 (Herms and McCullough 2014). This has resulted in the death of hundreds of millions of ash trees across the continent (McCullough 2019). Efforts to prevent the spread of the beetle have proved ineffective, with the beetle now ranging from British Columbia (Macquarrie et al. 2025) in Canada to Texas and Massachusetts (USDA 2025) in the USA. In part, this is due to the difficulty of detecting an EAB outbreak early, which is critical to maximise the likelihood of eradication (Alonso Chávez et al. 2026).

In Europe, the beetle was first detected in Moscow in 2007 (EPPO 2007) and has since spread to Ukraine (Drogvalenko et al. 2019), Belarus (EPPO 2025), Hungary (EPPO 2026a) and Slovakia (EPPO 2026b), now impacting trees that are also under stress by ADB (Davydenko et al. 2022). Research efforts are underway to understand the nature of the EAB-ADB interaction. Current studies have focused on understanding this relationship in the laboratory (Gossner et al. 2023) and through field observations (Davydenko et al. 2022), but critically, it is not known how ADB could affect the landscape-scale spread of EAB. This knowledge is urgently required to

93 understand the potential impacts of EAB on already weakened ADB trees, as well as where and
94 when surveillance and control strategies should be used.

95 Despite the initial detection of ADB in Great Britain (GB) in 2012, there is currently insufficient
96 spatio-temporal data on ADB arrival and progression that can be used to understand disease
97 impacts over time (Combes et al. 2024). Therefore, we constructed a compartmental model for
98 ADB in GB transitioning trees between disease severity categories under different disease
99 progress rate scenarios (i.e. the rate trees transition from asymptomatic, through canopy
100 decline to mortality), accounting for both environmental and tree stand characteristics to
101 provide spatial estimates of likely disease impacts. Next, using these spatial estimates, we
102 explore the influence of ADB co-occurring with EAB on ash trees, following a hypothetical EAB
103 invasion.

104 The overall aim of this study is to provide information on landscape scale impacts of ADB on
105 EAB spread, that can be used to guide future research and policy for effective EAB management
106 strategies. The specific objectives of this study are: (1) to provide landscape-scale estimates of
107 the distributions of ADB severity in GB in the absence of spatio-temporal survey data; (2) to
108 understand the most likely impacts of ADB on EAB spread; (3) to understand the factors that
109 can drive impacts of ADB on EAB spread.

110

111 Methods

112 Previous research developed an arrival, spread and detection model for EAB in GB to examine
113 the efficacy of different survey methods and optimise where to place them for early detection of
114 the beetle (Alonso Chávez et al. 2025). Here, we first construct a compartmental model to
115 estimate the distributions of ADB impacts on ash in GB at 1 km^2 resolution, and then adapt the

earlier EAB population dynamics model (Alonso Chávez et al. 2025) to include the modelled distributions of ADB to explore its impacts on EAB population dynamics in GB.

Compartmental model of ash dieback disease

The compartments in the ADB model were defined as: not noticeably diseased/ asymptomatic ash (S;crown dieback < ~15%), moderately diseased ash (E; crown dieback ~15-50%), heavily diseased ash (I; crown dieback ~ >50%), recently dead (within previous three years) (D), and removed ash (R) (Fig. 1). These broad ADB compartments were chosen based on available data sources as described below, and to provide the necessary resolution of ADB-induced stress on trees to model likely ADB impacts on EAB spread.

The model assumes a static population of ash and negligible recruitment into the population given a very high mortality rate of regenerating ash (Marçais et al. 2017). The model runs for a maximum of 27 years, i.e., the approximate generation time in European ash (San-Miguel-Ayanz et al. 2016), to avoid impacts of natural selection in regenerating ash (Metheringham et al. 2025) and impacts of climatic changes, which were not included in the ADB model to limit complexity in the absence of reliable datasets on the influence of future climate.

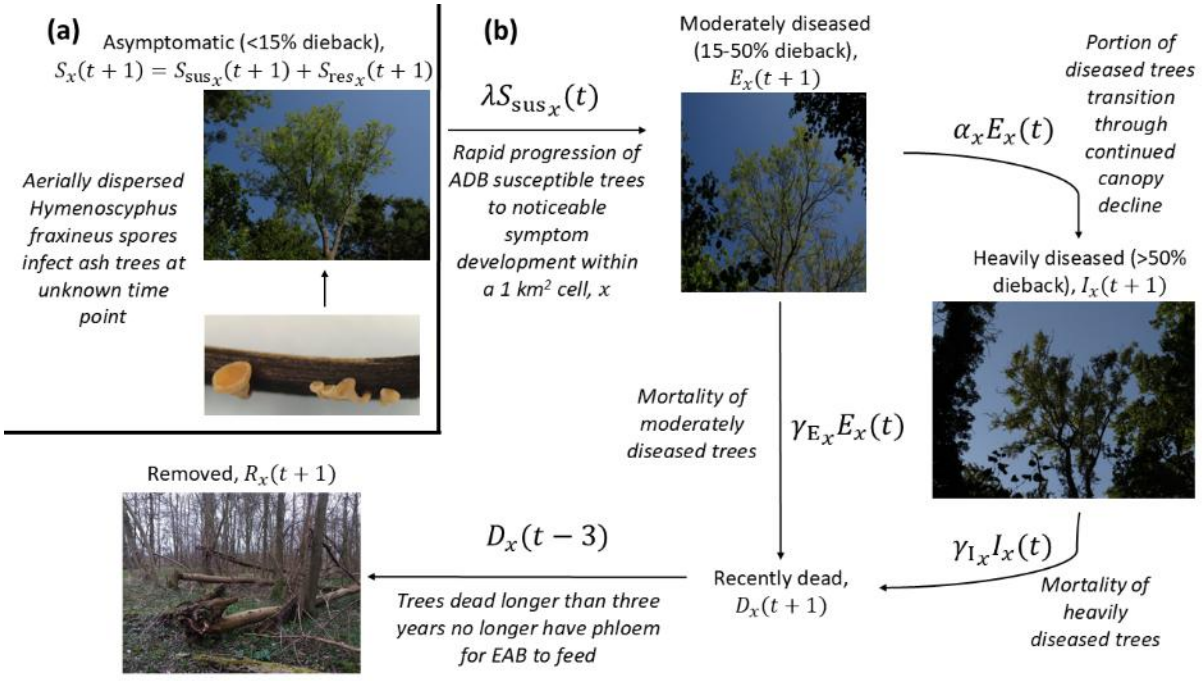


Fig. 1 Schematic concept of ADB compartmental model. (a) Representing the non-modelled lag period of the disease cycle where the causal agent of ADB is present for an unknown period prior to noticeable disease symptoms at a 1 km^2 grid cell, x, sufficient for detection. (b) The compartmental model begins following the end of the lag period, representing susceptible asymptomatic trees within a cell, $S_{\mathrm{sus}_x} = S_x - S_{\mathrm{res}_x}$, quickly transitioning to moderately diseased, E_x, at rate λ. A proportion of these trees, E_x, rapidly decline and die, D_x, at rate γ_{E_x}, while others transition to heavily diseased, I_x, at rate α_x. A portion of trees within the heavily diseased compartment, I_x, decline and die, D_x, at rate γ_{I_x}. Trees that have been dead for three years are removed, R_x. Mortality, γ_x, and ADB severity, α_x, transition parameters within a cell incorporate the impacts of soil moisture, precipitation and proportion of non-woodland trees, equation (9), with the model operating separately for mature and juvenile ash, equations (10-21)

Table 1. ADB compartmental model parameters, with symbols, values and sources.

168

Parameter	Symbol	Value	Source
Annual asymptomatic to moderately diseased transition rate	λ	0.5 yr^{-1}	Grosdidier et al., 2020
Initial proportion of ADB resistant ash	r_x	$\sim U(0.019, 0.055)$	Schertler et al., 2026
Baseline annual mature ash mortality transition rate (minimum, median, maximum estimates)	γ_{mat}	$\gamma_{\mathrm{mat}_{\mathrm{min}}} = 0.009\ yr^{-1}$ $\gamma_{\mathrm{mat}_{\mathrm{med}}} = 0.0205\ yr^{-1}$ $\gamma_{\mathrm{mat}_{\mathrm{max}}} = 0.032\ yr^{-1}$	Marçais et al., 2017; Klesse et al., 2021; George et al., 2022
Initial proportion of ash in maturity classes (juvenile (< 20 cm dbh); mature (> 20 cm dbh))	κ	$\kappa_{\mathrm{juv}} = 0.71$ (initial value) $\kappa_{\mathrm{mat}} = 0.29$ (initial value)	Forestry Commission 2013
Mortality transition rate multiplier for juvenile ash	c	3.125	Marçais et al., 2017
Mortality transition rate multiplier for heavily diseased ash, I, compared to moderately diseased ash, E	d	3	Value varies depending on q (fitted using Timmermann et al., 2017)
Scaling factor to estimate transition rate from moderately diseased to heavily diseased ash from the mortality transition rates	q	$q_{\mathrm{mat}} = 0.724$ $q_{\mathrm{juv}} = 0.712$	Timmermann et al., 2017
Proportion of trees in non-woodland environments	ζ_x	Cell, x, specific	Brown et al., 2023
Non-woodland mortality transition rate reduction factor	h	0.537	Laubray et al., 2023
Soil moisture adjusted mortality transition rate multiplier (none, minimum, median, maximum estimates)	μ_x	$\mu_{\mathrm{notwet}} = 1$ $\mu_{\mathrm{minwet}} = 1.857$ $\mu_{\mathrm{medwet}} = 1.9505$ $\mu_{\mathrm{maxwet}} = 2.04$	Pušpure et al., 2017; Klesse et al., 2021
Local precipitation difference from minimum mean value in cell with ash in Britain (620 mm yr^{-1})	ρ_x	Cell, x, specific (mm yr^{-1})	Wouters 2021
Proportional mortality transition rate increase mm^{-1} yr^{-1} precipitation	ϕ	0.0004 mm^{-1} yr^{-1}	Klesse et al., 2021

169 ***Ash dieback arrival***

It is necessary to estimate the arrival year of the pathogen or first ADB symptoms across GB to provide a date to begin a compartmental model. The absence of reliable data on pathogen presence and the disease lag phase throughout Europe means the model starts upon detection of trees with noticeable disease symptoms E (Fig. 1). The first model transition to diseased ash, (from S to E), occurred in 2012 following the first detection of ash dieback disease in the GB. In 2012, following this initial disease detection, a survey of 2500 sites across Britain in each 10 km^2 area where ash was known to be present was undertaken. From this point onwards, disease detection data becomes unreliable due to dependency on public reporting. Therefore, in accordance with the disease front spread rate from Norwegian data (Børja et al. 2017), we consider trees to transition to E, at an outward spread rate of 50 km year^{-1} from the initial 2012-13 disease detection locations. Once moderately diseased trees E are present in a cell, x, ADB susceptible asymptomatic trees, S_{sus_x}, rapidly transition to E_x at a rate of λ (Grosdidier et al. 2020) (Fig. 1). It is estimated the proportion of minimally affected, or resistant ash, r, to ADB is between 0.019 to 0.055 (Schertler et al., 2026). Therefore, for each cell, the proportion of resistant ash originally present within a cell, r_x was randomly sampled from a uniform distribution between 0.019 and 0.055, $r_x \sim U(0.019, 0.055)$, with resistant trees, S_{res_x}, remaining ADB asymptomatic throughout the model, $S_x = S_{\mathrm{sus}_x} + S_{\mathrm{res}_x}$. Trees affected by ADB then either rapidly decline and die (frequently associated with secondary pathogenic *Armillaria* spp. (Combes et al. 2024)) or continue to progress through a canopy decline (Fig. 1).

Canopy decline

The rate of canopy decline was then estimated to enable modelling of the distribution of the ADB stress categories (E, I) that EAB will interact with. Once trees are E, they transition to I, at a rate α, to represent the process of continued *H. fraxineus* induced canopy decline. The absence of data on the transition of ash between disease severity categories through time meant that the

transition rate, α, of ash from moderately diseased, E, to heavily diseased, I, was estimated by dividing the mortality transition rate, γ, by a scaling factor, q, for both mature, q_{mat}, and juvenile ash, q_{juv} to produce field-realistic disease severity distributions:

$$\alpha_{\mathrm{mat}_x} = \frac{\gamma_{\mathrm{mat}_x}}{q_{\mathrm{mat}}} \quad (1)$$

$$\alpha_{\mathrm{juv}_x} = \frac{\gamma_{\mathrm{juv}_x}}{q_{\mathrm{juv}}} \quad (2)$$

We use a scenario based on Norwegian survey data (Timmermann et al., 2017) to estimate, q_{mat} and q_{juv}. The compartmental model (Fig. 1) was run for 10 years and the L-BFGS-B algorithm (Byrd et al. 1995) via the optim function of the stats package in R software version 4.1.2 (R Core Team 2025) was used to minimise the sum of square relative deviations to provide estimates for q_{juv} and q_{mat}, for combinations of 22% mature ash mortality and 20% highly diseased mature ash, and 42% juvenile ash mortality and 26% highly diseased juvenile ash ten years after disease arrival (Figs. 2b,c in Timmermann et al., 2017). This resulted in values $\alpha_{\mathrm{mat}_x} = 0.724$ and $\alpha_{\mathrm{juv}_x} = 0.712$.

Mortality

The mortality probability of trees dependent on canopy status is not known. Separate mortality transition parameters were provided for E, γ_{E}, and I, γ_{I}, ash to provide a more realistic model description of the disease process. The mortality transition rate for I trees, γ_{I}, was specified three times ($d = 3$) the mortality transition rate for E trees, γ_{E}, whilst the overall mortality transition rate for a cell, γ_x, remained constant:

$$\gamma_x = \frac{\gamma_{\mathrm{E}_x} E_x + \gamma_{\mathrm{I}_x} I_x}{E_x + I_x} \quad (3)$$

$$\gamma_{\mathrm{I}_x} = d\gamma_{\mathrm{E}_x} \quad (4)$$

$$\gamma_{\mathrm{E}_x} = \gamma_x \frac{E_x + I_x}{E_x + dI_x} \quad (5)$$

The chosen d value does not impact distributions of canopy status because q_{mat} and q_{juv} were parameterised (see above) using a value of $d = 3$, with q and d values interdependent and not separately identifiable from Timmermann et al. (2017).

The ADB mortality transition parameter for mature ash (> 20 cm dbh), γ_{mat} was obtained from studies which surveyed multiple stands over large geographic areas, avoiding estimates that were bias by site specific conditions or bias towards ash dominated stands or plantations (Marçais et al., 2017; Klesse et al., 2021; George et al., 2022). Bias towards surveying ash dominated stands was common in the literature, and at the time of review, only three papers deemed to provide reliable 'baseline' estimates for annual mature ash mortality were identified (Marçais et al., 2017; Klesse et al., 2021; George et al., 2022). These provided a lower γ_{mat} estimate of 0.009 (Klesse et al. 2021), an upper γ estimate of 0.032 (Marçais et al. 2017), and a median γ_{mat} estimate of 0.0205. For juvenile ash trees (i.e. < 20 cm dbh), the mature ash mortality transition parameter γ_{mat} was adjusted by multiplying by an additional juvenile mortality multiplier c. This was estimated using data from Marçais et al. (2017) demonstrating that the annual juvenile mortality rate is 3.125 times the annual adult mortality rate:

$$\gamma_{\mathrm{juv}} = c\gamma_{\mathrm{mat}} \quad (6)$$

Environment and stand impacts

For each 1 km x 1km grid cell, x, in the model, γ and α were adjusted based on environmental and stand characteristics to produce cell specific mortality γ_x, and ADB severity, α_x, transition parameters. Parameters were conservatively adjusted for environmental impacts by using the overall percentage differences in disease due to environmental impacts quantified from available literature (see below). This approach was used to prevent overestimates of ADB

241 progression from environmental impacts and thus, overestimates of how ADB could impact EAB
242 in the absence of data to quantify how these impacts vary through time, particularly given
243 reports of ADB severity stabilising (Laubray et al. 2023; Fuchs et al. 2024).

244 The most influential factors on ADB development are moisture, the presence of temperatures
245 above 28°C, the density, and age of ash (Combes et al. 2024). The presence of temperatures
246 above 28°C was not included because this temperature is not currently routinely reached in GB.
247 Additionally, we assumed no spatial bias at the landscape scale of the density of ash within
248 stand environments. Forestry Commission NFI data (Forestry Commission 2013) were used to
249 provide initial national proportion estimates of 0.71 juvenile ash, κ_{juv}, and 0.29 mature ash,
250 κ_{mat}, which changed as trees were removed from the landscape.

251 The site soil moisture mortality factor, μ, was established through a literature search providing
252 quantitative values of differences in ADB severity for trees on 'wet soil' sites. This provided
253 estimates of a 104% increase in the probability that trees were classified as not healthy on a wet
254 site eight years after disease arrival (Pušpure et al. 2017), and an increase in mortality
255 probability of 85.7% between 2009-2019 (Klesse et al. 2021).

256 Grid cells were classified as wet by meeting two criteria: (1) they were in the top third for the
257 mean annual gravimetric soil water content in the top soil layer and (2) if the dominant soil type
258 was classified as either imperfectly drained, poorly drained, or very poorly drained (FAO and
259 IIASA 2023). This resulted in 22.5% of grid cells containing ash classified as 'wet' locations.
260 Gravimetric soil water content was estimated using the volumetric soil water content (0 - 7 cm)
261 (Wouters 2021) and reference bulk density (< 20 cm depth) (FAO and IIASA 2023) to characterise
262 relative wetness across cells. As volumetric soil water content more directly reflects soil
263 saturation, we confirmed that using volumetric rather than gravimetric values resulted in
264 negligible differences in the cells classified as wet.

The effect of precipitation was determined from a quantitative estimate of the impact of precipitation on annual ash mortality from the Swiss NFI with a range of annual precipitation values from 618 to 2191 mm year^{-1} that is comparable to values in GB (UK Met Office 2025), whilst accounting for other variables that influenced ash mortality (Klesse et al. 2021). The precipitation adjusted mortality transition (mm^{-1}) (Klesse et al. 2021) (Table 1) were then used along with the mean annual precipitation and standard deviation to estimate an additional impact of ~ 0.04% in mortality probability per additional mm year^{-1} of rain, ϕ. The cell specific precipitation mortality factor, τ_x, was calculated using the difference from the minimum mean annual precipitation value in Great Britain (620 mm (Wouters 2021)) in a cell with ash, ρ_x:

$$\tau_x = 1 + \phi\rho_x \quad (7)$$

Trees in non-woodland environments have approximately 54% less ($h = 0.54$) of the mean ADB crown decline of woodland trees approximately 10 years after disease arrival (Laubray et al. 2023). The proportion of ash in non-woodland environments in a cell ζ_x, was calculated in each 1 km^2 cell from the map of ash tree density across GB (Brown et al. 2023) from the data that were then used to construct the map as the proportion of trees that were in urban environments, open land environments, or small woody features. The non-woodland mortality factor υ_x was then calculated by multiplying the proportion of trees in non-wood environments ζ_x, by the reduction in ADB severity for non-woodland trees h:

$$\upsilon_x = h\zeta_x \quad (8)$$

This can be summarised together to obtain the cell specific mortality transition parameter as:

$$\gamma_x = \gamma(\tau_x + \mu_x - 1)(1 - \upsilon_x) \quad (9)$$

Model transitions

The model operates separately for mature and juvenile ash within a cell and provides an estimate for ash across all age categories for transitions between model compartments. The system dynamics are given by:

$$E_{\mathrm{mat}_x}(t+1) = E_{\mathrm{mat}_x}(t) + \lambda S_{\mathrm{sus}_{\mathrm{mat}_x}}(t) - \alpha_{\mathrm{mat}_x} E_{\mathrm{mat}_x}(t) - \gamma_{\mathrm{mat}_{\mathrm{E}_x}} E_{\mathrm{mat}_x}(t) \quad (10)$$

$$E_{\mathrm{juv}_x}(t+1) = E_{\mathrm{juv}_x}(t) + \lambda S_{\mathrm{sus}_{\mathrm{juv}_x}}(t) - \alpha_{\mathrm{juv}_x} E_{\mathrm{juv}_x}(t) - c\gamma_{\mathrm{juv}_{\mathrm{E}_x}} E_{\mathrm{juv}_x}(t) \quad (11)$$

$$E_x(t+1) = \kappa_{\mathrm{mat}} E_{\mathrm{mat}_x}(t+1) + \kappa_{\mathrm{juv}} E_{\mathrm{juv}_x}(t+1) \quad (12)$$

$$I_{\mathrm{mat}_x}(t+1) = I_{\mathrm{mat}_x} + \alpha_{\mathrm{mat}_x} E_{\mathrm{mat}_x}(t) - \gamma_{\mathrm{mat}_{\mathrm{I}_x}} I_{\mathrm{mat}_x}(t) \quad (13)$$

$$I_{\mathrm{juv}_x}(t+1) = I_{\mathrm{juv}_x} + \alpha_{\mathrm{juv}_x} E_{\mathrm{juv}_x}(t) - c\gamma_{\mathrm{juv}_{\mathrm{I}_x}} I_{\mathrm{juv}_x}(t) \quad (14)$$

$$I_x(t+1) = \kappa_{\mathrm{mat}_x} I_{\mathrm{mat}_x}(t+1) + \kappa_{\mathrm{juv}_x} I_{\mathrm{juv}_x}(t+1) \quad (15)$$

$$D_{\mathrm{mat}_x}(t+1) = D_{\mathrm{mat}_x}(t) + \gamma_{\mathrm{mat}_{\mathrm{E}_x}} E_{\mathrm{mat}_x}(t) + \gamma_{\mathrm{mat}_{\mathrm{I}_x}} I_{\mathrm{mat}_x}(t) - D_{\mathrm{mat}_x}(t-3) \quad (16)$$

$$D_{\mathrm{juv}_x}(t+1) = D_{\mathrm{juv}_x}(t) + c\gamma_{\mathrm{juv}_{\mathrm{E}_x}} E_{\mathrm{juv}_x}(t) + c\gamma_{\mathrm{juv}_{\mathrm{I}_x}} I_{\mathrm{juv}_x}(t) - D_{\mathrm{juv}_x}(t-3) \quad (17)$$

$$D_x(t+1) = \kappa_{\mathrm{mat}_x} D_{\mathrm{mat}_x}(t+1) + \kappa_{\mathrm{juv}_x} D_{\mathrm{juv}_x}(t+1) \quad (18)$$

$$R_{\mathrm{mat}_x}(t+1) = R_{\mathrm{mat}_x}(t) + D_{\mathrm{mat}_x}(t-3) \quad (19)$$

$$R_{\mathrm{juv}_x}(t+1) = R_{\mathrm{juv}_x}(t) + D_{\mathrm{juv}_x}(t-3) \quad (20)$$

$$R_x(t+1) = \kappa_{\mathrm{mat}_x} R_{\mathrm{mat}_x}(t+1) + \kappa_{\mathrm{juv}_x} R_{\mathrm{juv}_x}(t+1) \quad (21)$$

EAB arrival and spread model

The model of EAB arrival and spread in Britain was adapted from Alonso Chávez et al. (2025) to interact with the ADB compartmental model. Trees killed by ADB for more than three years were removed from the landscape to conservatively account for tree phloem desiccation of dead trees, with previous work demonstrating larvae can still emerge from infested logs cut the previous year (Petrice and Haack 2007). The model used in this study assumes a 70% confidence that invasions would come through known firewood import pathways, and a 50% probability of EAB escaping at ports and 50% at depots.

ADB impact on the population dynamics of EAB

Based on previous research in North America (Mercader et al. 2011a; Jennings and Shrewsbury 2015) and early survey reports from Ukraine, a baseline scenario is specified with diseased trees within a cell (E_x and I_x) considerably more attractive to EAB than trees that are either asymptomatic, S_x, or recently dead D_x. Current evidence from within Ukraine (personal communication) also suggests that among ADB infected trees, heavily diseased trees, I, attract beetles at a lower rate than moderately symptomatic trees, E. This means that E trees are more likely to become infested, G, and less likely to remain uninfested, U, than I trees. Using field data from 16 sites in Michigan, Mercader et al. (2011a) provide an equation to estimate the ratio of larval density on girdled over non-girdled trees, from the larval density on non-girdled trees:

$$y = 20.468x^{-0.559} \quad (22)$$

We used this equation to estimate an EAB attraction multiplier for E_x and I_x trees from the larval density on the remaining S_x and D_x trees in a cell, L_{SD_x}. To account for a weaker attractive effect of I trees compared to E trees, we assume that EAB are attracted to I_x ash within a cell by a multiplier, η_{I_x}, that is half the multiplier for E_x ash within a cell, η_{E_x}:

$$\eta_{\mathrm{E}_x} = 20.468 L_{\mathrm{SD_x}}^{-0.559} \quad (23)$$

$$\eta_{\mathrm{I}_x} = \frac{20.468 L_{\mathrm{SD_x}}^{-0.559}}{2} \quad (24)$$

The probability of trees in a cell remaining uninfested, U_x, can be calculated using the probability of an EAB egg laid on a previously uninfested tree ($\psi = 0.0001$) and the number of adult EAB in a cell A_x:

$$U_x(t+1) = U_x(t) e^{-\psi A_x(t)} \quad (25)$$

The trees within a cell in ADB severity category E_x are η_{E_x} times as likely to become infested as S_x or D_x trees, and trees in ADB severity category I_x are η_{I_x} times as likely to become infested as S_x or D_x trees, whilst the overall probability that trees within a cell become infested (G_x) is not affected in the presence of available uninfested hosts in ADB severity categories:

$$G_{\mathrm{S}_x}(t+1) = G_{\mathrm{S}_x}(t) + U_{\mathrm{S}_x}(t)(1 - e^{-\psi A_x(t)}) \left[\frac{U_{\mathrm{S}_x}(t) + U_{\mathrm{E}_x}(t) + U_{\mathrm{I}_x}(t) + U_{\mathrm{D}_x}(t)}{U_{\mathrm{S}_x}(t) + \eta_{\mathrm{E}_x} U_{\mathrm{E}_x}(t) + \eta_{\mathrm{I}_x} U_{\mathrm{I}_x}(t) + U_{\mathrm{D}_x}(t)} \right] (26)$$

$$G_{\mathrm{E}_x}(t+1) = G_{\mathrm{E}_x}(t) + \eta_{\mathrm{E}_x} U_{\mathrm{E}_x}(t)(1 - e^{-\psi A_x(t)}) \left[\frac{U_{\mathrm{S}_x}(t) + U_{\mathrm{E}_x}(t) + U_{\mathrm{I}_x}(t) + U_{\mathrm{D}_x}(t)}{U_{\mathrm{S}_x}(t) + \eta_{\mathrm{E}_x} U_{\mathrm{E}_x}(t) + \eta_{\mathrm{I}_x} U_{\mathrm{I}_x}(t) + U_{\mathrm{D}_x}(t)} \right] (27)$$

$$G_{\mathrm{I}_x}(t+1) = G_{\mathrm{I}_x}(t) + \eta_{\mathrm{I}_x} U_{\mathrm{I}_x}(t)(1 - e^{-\psi A_x(t)}) \left[\frac{U_{\mathrm{S}_x}(t) + U_{\mathrm{E}_x}(t) + U_{\mathrm{I}_x}(t) + U_{\mathrm{D}_x}(t)}{U_{\mathrm{S}_x}(t) + \eta_{\mathrm{E}_x} U_{\mathrm{E}_x}(t) + \eta_{\mathrm{I}_x} U_{\mathrm{I}_x}(t) + U_{\mathrm{D}_x}(t)} \right] (28)$$

$$G_{\mathrm{D}_x}(t+1) = G_{\mathrm{D}_x}(t) + U_{\mathrm{D}_x}(t)(1 - e^{-\psi A_x(t)}) \left[\frac{U_{\mathrm{S}_x}(t) + U_{\mathrm{E}_x}(t) + U_{\mathrm{I}_x}(t) + U_{\mathrm{D}_x}(t)}{U_{\mathrm{S}_x}(t) + \eta_{\mathrm{E}_x} U_{\mathrm{E}_x}(t) + \eta_{\mathrm{I}_x} U_{\mathrm{I}_x}(t) + U_{\mathrm{D}_x}(t)} \right] (29)$$

$$G_x = G_{S_x} + G_{E_x} + G_{I_x} + G_{D_x} \quad (30)$$

An additional attraction of EAB to E_x and I_x trees in a cell results in different larval, L_x, and adult EAB, A_x, densities on trees in a cell depending on their ADB severity category. Adult EAB are also η_{E_x} times as likely to have laid eggs on a G_{E_x} tree within a cell and η_{I_x} times as likely to have laid eggs on a G_{I_x} tree within a cell in comparison to a G_{S_x} or G_{D_x} tree. This therefore impacts density dependent parameters in the EAB population dynamics model such as the density dependent mortality rate of larvae, the number of EAB emerging from an infested tree and the number of overwintering larvae.

In the baseline scenario for ADB impacts on EAB, the mortality rates of EAB larvae attributed to host resistance were not adjusted according to ADB severity. Subsequently, this assumption was explored by varying the density-independent larval death rate, ω, which was calculated as a daily mortality rate (0.2) from the overall 56-day larval development time, T (Alonso Chávez et al. 2025). An ADB severity adjusted ω value, ω_{ADB}, was calculated for each ADB severity category by dividing the density-independent larval death rate, ω, by realistic values determined from the impacts of host drought stress on EAB larval mortality (Showalter et al. 2018), ϵ_{ADB}, which decreased larval mortality on E, I, D trees by a factors of up to ~3 (Showalter et al. 2018) relative to S trees:

$$\omega_{\mathrm{ADB}_x} = \frac{\omega_x}{\epsilon_{\mathrm{ADB}}} \quad (31)$$

Simulated scenarios

ADB model

The ADB compartmental model was examined in the absence of EAB to estimate the proportion of trees the different ADB model compartments in 2026 and 2039 with separate scenarios using the low, median and high estimates of ADB progress.

ADB impact on EAB spread

Given the uncertainty in the current interaction between ADB and EAB, nine post-EAB arrival scenarios were assessed to examine i) the impact of differences in beetle attraction to ADB affected trees, ii) larval mortality on ADB affected trees, iii) EAB arrival year and iv) ADB progress rate (Table 2). For each scenario, 9993 model iterations were performed, with the spread of EAB recorded up to eight years after the arrival event. Data were visualised using the ggplot2 package (Wickham 2016) using R software version 4.1.2 (R Core Team 2025). Artificial intelligence large language model (Claude, Anthropic) was used for assistance with code debugging and the replacement of NAG library software within the Alonso Chávez et al. (2025) EAB population dynamics model with either GNU Scientific Library version 2.8 (Galassi et al., 2009) or analytical solutions. These changes were validated against the original model.

397

398

399 **Table 2.** Scenarios of ADB impact on EAB spread in GB up to eight years after beetle arrival.

Parameter examined	EAB arrival year	ADB rate[a]	EAB attraction	Larval mortality
Baseline	2026	Median	Baseline $\eta_{\mathrm{E}} = 20.468L_{\mathrm{SD}}^{-0.559}$ $\eta_{\mathrm{I}} = \frac{20.468L_{\mathrm{SD}}^{-0.559}}{2}$	Baseline $\epsilon_{\mathrm{ADB}} = 1$
Attraction	2026	Median	Half baseline $\eta_{\mathrm{E}} = \frac{20.468L_{\mathrm{SD}}^{-0.559}}{2}$ $\eta_{\mathrm{I}} = \frac{20.468L_{\mathrm{SD}}^{-0.559}}{4}$	Baseline $\epsilon_{\mathrm{ADB}} = 1$
Attraction	2026	Median	Quarter baseline $\eta_{\mathrm{E}} = \frac{20.468L_{\mathrm{SD}}^{-0.559}}{4}$ $\eta_{\mathrm{I}} = \frac{20.468L_{\mathrm{SD}}^{-0.559}}{8}$	Baseline $\epsilon_{\mathrm{ADB}} = 1$
Attraction	2026	Median	No difference $\eta_{\mathrm{E}} = 1$ $\eta_{\mathrm{I}} = 1$	Baseline $\epsilon_{\mathrm{ADB}} = 1$
Larval mortality (Scenario 1)	2026	Median	Baseline $\eta_{\mathrm{E}} = 20.468L_{\mathrm{SD}}^{-0.559}$ $\eta_{\mathrm{I}} = \frac{20.468L_{\mathrm{SD}}^{-0.559}}{2}$	$\epsilon_{\mathrm{S}} = 1$ $\epsilon_{\mathrm{E}} = 1.17$ $\epsilon_{\mathrm{I}} = 1.33$ $\epsilon_{\mathrm{D}} = 1.5$
Larval mortality (Scenario 2)	2026	Median	Baseline $\eta_{\mathrm{E}} = 20.468L_{\mathrm{SD}}^{-0.559}$ $\eta_{\mathrm{I}} = \frac{20.468L_{\mathrm{SD}}^{-0.559}}{2}$	$\epsilon_{\mathrm{S}} = 1$ $\epsilon_{\mathrm{E}} = 1.66$ $\epsilon_{\mathrm{I}} = 2.33$ $\epsilon_{\mathrm{D}} = 3$
EAB arrival date	2031	Median	Baseline $\eta_{\mathrm{E}} = 20.468L_{\mathrm{SD}}^{-0.559}$ $\eta_{\mathrm{I}} = \frac{20.468L_{\mathrm{SD}}^{-0.559}}{2}$	Baseline $\epsilon_{\mathrm{ADB}} = 1$
ADB progress	2026	Low	Baseline $\eta_{\mathrm{E}} = 20.468L_{\mathrm{SD}}^{-0.559}$ $\eta_{\mathrm{I}} = \frac{20.468L_{\mathrm{SD}}^{-0.559}}{2}$	Baseline $\epsilon_{\mathrm{ADB}} = 1$
ADB progress	2026	High	Baseline $\eta_{\mathrm{E}} = 20.468L_{\mathrm{SD}}^{-0.559}$ $\eta_{\mathrm{I}} = \frac{20.468L_{\mathrm{SD}}^{-0.559}}{2}$	Baseline $\epsilon_{\mathrm{ADB}} = 1$

[a]See Table 1 for parameter values of the ADB model. Median ADB progress rate uses 'median' parameter values, Low ADB progress rate uses 'minimum' parameter values, High ADB progress rate uses 'maximum' parameter values.

Results

To enable appropriate interpretation the impacts of ADB on EAB spread in GB, we first describe the distributions of ADB impacts on ash (S, E, I, D, R trees) from the ADB compartmental model prior to examining the impacts of ADB on the population dynamics of EAB.

Exploring ash dieback impacts in Britain

The proportion of removed ash trees varied spatially, increased through time, and were heavily dependent on both the age of trees and the rate of ADB progress (Figs. 2-3; Online Resource 1, Figs. S37-S38). At the median rate of ADB progress, in 2026, the median value of R was 0.264 (min = 0.093, max = 0.602), and increased to 0.543 (min = 0.329, max = 0.855) by 2039. The value of R was smaller for the low ADB progression rate scenario (2026 median = 0.126, min = 0.042, max = 0.335; 2039 median = 0.302, min = 0.163, max = 0.635), and larger for the high ADB progression rate scenario (2026 median = 0.378, min = 0.141, max = 0.750; 2039 median = 0.686, min = 0.456, max = 0.917). A larger proportion of juvenile trees rather than mature trees were R, and this difference between juvenile and mature trees increased through time and with a quicker rate of ADB progress (Figs. 2-3; Online Resource 1, Figs. S37-S38).

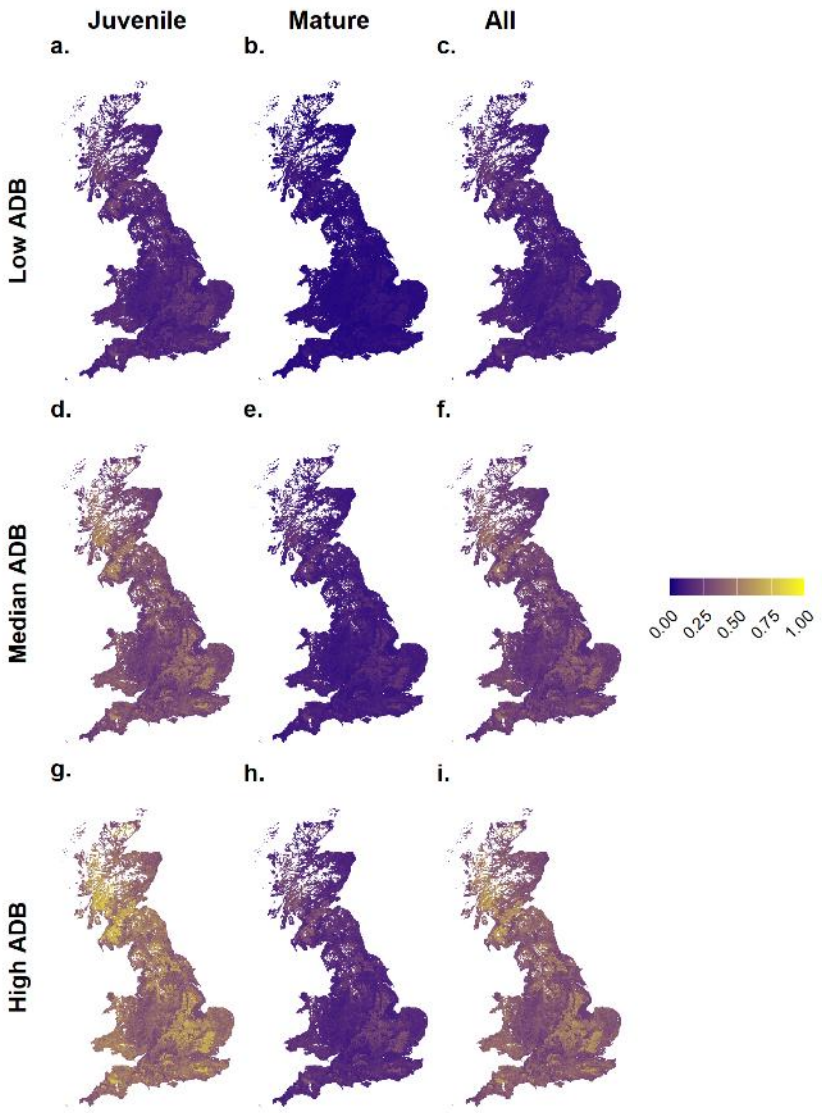


Fig. 2 Modelled proportion of ash that are removed by ADB across GB by 2026 under different ADB progression scenarios (Low: (a), (b), (c); Median (d), (e), (f); High (g), (h), (i)) and for different age categories (Juvenile (7-20 cm dbh): (a), (d), (g); Mature (> 20 cm dbh): (b), (e), (h); All (≥ 7 cm dbh): (c), (f), (i))

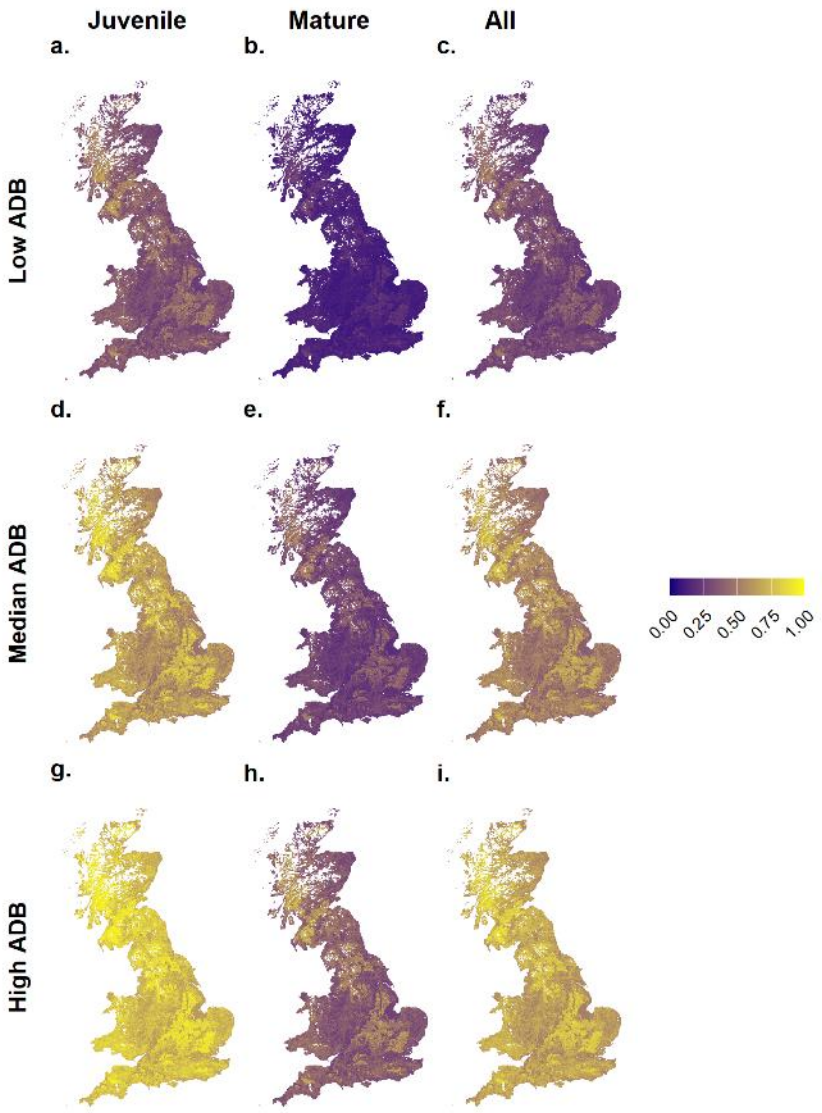


Fig. 3 Modelled proportion of ash that are removed by ADB across GB by 2039 under different ADB progression scenarios (Low: (a), (b), (c); Median (d), (e), (f); High (g), (h), (i)) and for different age categories (Juvenile (7-20 cm dbh): (a), (d), (g); Mature (> 20 cm dbh): (b), (e), (h); All (≥ 7 cm dbh): (c), (f), (i))

By 2026, only a small proportion of remaining ash trees in the landscape were in the asymptomatic compartment S (median = 0.051, min = 0.043, max = 0.093). Almost all remaining trees transitioned into the ADB symptomatic compartments (E, I, D), with the proportion of trees in each compartment varying spatially (Online Resource 1, Fig. S1). In 2026, under the median estimated rate of ADB progress, most ash were E (median = 0.527, min = 0.247, max = 0.717), followed by I (median = 0.313, min = 0.172, max = 0.420) and then D (median = 0.109, min = 0.065, max = 0.283) (Online Resource 1, Figs. S1-S2). By 2039, model transitions resulted in slightly higher median I ash (0.450) compared to E (0.374), although the variation in E ash (min = 0.150, max = 0.536) was greater than I (min = 0.344, max = 0.482) (Online Resource 1, Figs. S3-S4). The proportion of D ash remained relatively stable (median = 0.095, min = 0.060, max = 0.161), whilst asymptomatic S ash increased slightly as non-resistant trees were removed (median = 0.081, min = 0.055, max = 0.256) (Online Resource 1, Figs. S3-S4).

More juvenile ash were D than mature ash (Online Resource 1, Figs. S5-S12, S17-S24, S29-S36), and juvenile ash also transitioned quicker from E to I. The proportion of S trees were greater among juvenile ash and increased more through time as non-resistant trees were removed at a quicker rate (Online Resource 1, Figs. S5-S12, S17-S24, S29-S36). Similarly, for the high ADB progression rate scenario, a larger proportion of ash were D and transitioned quicker from E to I, whilst the proportion of S ash was greater and increased more through time as non-resistant trees were removed at a higher rate (Online Resource 1, Figs. S13-S36).

The influence of ADB on an EAB invasion in Britain

Baseline scenario

The baseline ADB scenario resulted in a reduction in the number of cells colonised by EAB (Fig. 4a,b). Eight years after EAB arrival, a median number of 322 cells (5th percentile = 95, 1 cells; 95th percentile = 480 cells) were colonised when including the impact of ADB, compared to 368 cells (5th percentile = 160 cells; 95th percentile = 524 cells) when excluding the impact of ADB.

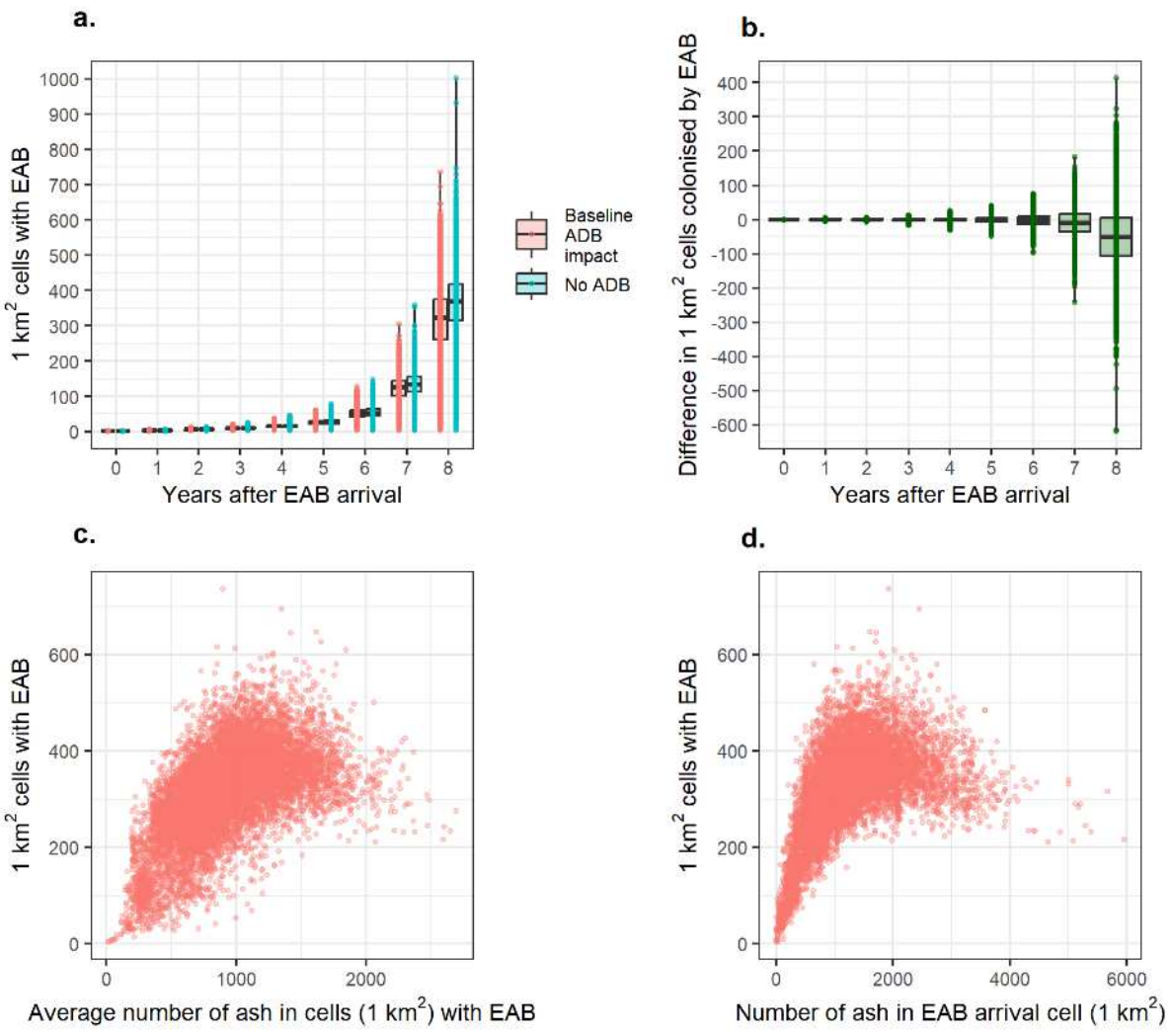


Fig. 4 ADB impacts on EAB spread under the baseline ADB scenario (Table 2) for each of the 9993 model iterations. (a) Boxplot of the number of 1 km^2 cells colonised by EAB with and without the baseline ADB scenario up to eight years after EAB arrival; (b) the number of 1 km^2 cells colonised by EAB under the baseline ADB scenario compared to no ADB; (c) the relationship between the average number of ash in cells up to seven years after EAB arrival and the number of 1 km^2 cells colonised by EAB eight years after EAB arrival for the baseline ADB

scenario; (d) the relationship between the number of ash in initial EAB arrival cell and the number of 1 km^2 cells with EAB eight years after beetle arrival for the baseline ADB scenario

ADB therefore also impacted the probability that a cell would be colonised within eight years should EAB arrive in Britain (Online Resource 1, Figs. S39-S40), with 56% of cells containing ash having a reduced probability of EAB colonisation in comparison to 24% having an increased probability of colonisation, while 20% remained unchanged. This therefore increased the proportion of cells with ash that were not colonised by EAB during any of the 9993 model iterations, from 7.3% to 9.6% when including the baseline ADB scenario (Online Resource 1, Fig. S40). Locations where EAB was no longer recorded were mainly spatially clustered in Scotland, Wales and northern (Cumbria and Northumberland) England, with some locations also present in eastern and southwest England (Online Resource 1, Fig. S40).

On average, the impacts of ADB on EAB spread begin to become apparent seven years after EAB arrival (11 km median difference) (Fig. 4a,b). However, the impacts of ADB vary depending on model iteration, and variation became greater with further median beetle spread (Fig. 4a,b). This variation between iterations can partially be explained by EAB model stochasticity and the large number of cells with a low probability of EAB presence eight years after an EAB arrival. Notably, the total number of cells colonised by EAB was strongly positively related to both the average number of ash in cells that EAB colonised (Fig. 4c), and the density of ash in the EAB arrival location (Fig. 4d).

Exploring the impact of model parameters on EAB invasion

In all examined scenarios, on average, the impact of ADB on EAB spread did not begin to become apparent until at least six years after EAB arrival (Figs. 5-7), with differences in the absence of EAB during any of the 9993 model realisations again mainly spatially clustered in

Scotland, Wales and northern (Cumbria and Northumberland) England, with some locations also present in eastern and southwest England (Online Resource 1, Figs. S43, S45, S47, S49, S51, S53, S55, S57).

Exploring the impact of EAB population dynamics parameters

The impact of reducing the attraction of EAB to stressed trees had negligible impact on EAB spread at both half and quarter the attraction rate compared to the baseline attraction scenario, although no EAB preference for ADB stressed trees did slightly increase beetle spread eight years after EAB arrival (median = 14 cells; 5th percentile = -129 cells; 95th percentile = 162 cells) (Online Resource 1, Figs. S41-S47).

In contrast, EAB spread rate increased when the mortality of EAB larvae on E, I, D trees relative to S trees were decreased by factors of 1.17, 1.33, 1.5 (larval mortality scenario 1, Table 2) or 1.66, 2.33, 3 respectively (larval mortality scenario 2, Table 2). EAB spread a median additional 52 cells (5th percentile = -88 cells; 95th percentile = 224 cells) after eight years under larval mortality scenario 1, and a median additional 155 cells (5th percentile = -20 cells; 95th percentile = 380 cells) under larval mortality scenario 2 in comparison to the baseline scenario (Fig. 5). This increased the probability of EAB presence for 56% of cells with ash (decreased for 23%; unchanged for 21%) for larval mortality scenario 1 and for 74% of cells with ash (decreased for 9%; unchanged for 17%) for larval mortality scenario 2 and therefore decreased the number of cells with ash that recorded no EAB during any iteration to 8.8% for larval mortality scenario 1 and 7.6% for larval mortality scenario 2 (Online Resource 1, Figs. S48-S51).

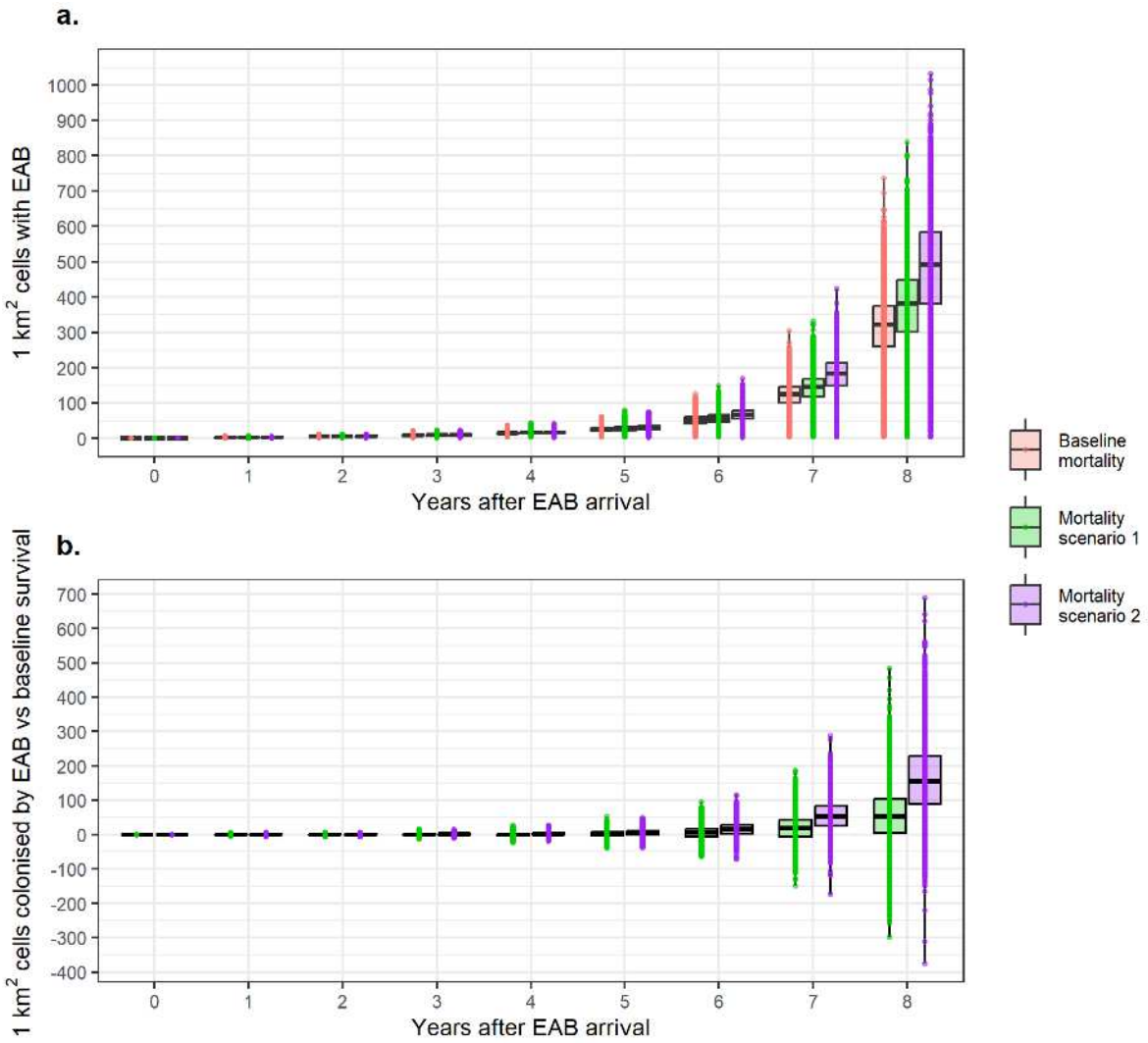


Fig. 5 Impact of EAB larval mortality rates on EAB spread for each of the 9993 model iterations. Baseline mortality represents equal density independent EAB larval mortality on $S, E, I\ D$ ash (Table 2); mortality scenario 1 represents a decrease in EAB larval mortality by factors of 1.17, 1.33, 1.5 for E, I, D ash relative to S ash (Table 2); mortality scenario 2 represents a decrease in EAB larval mortality by factors of 1.66, 2.33, 3 for E, I, D ash relative to S ash (Table 2). (a) Boxplot of the number of 1 km^2 cells colonised by EAB for each scenario up to eight years after

EAB arrival; (b) the number of 1 km^2 cells colonised by EAB under mortality scenarios 1 and 2 compared to the baseline scenario

Exploring the impact of EAB arrival date

EAB arrival in 2031 resulted in a slower spread of EAB in comparison to arrival in 2026, with a median difference of -22 (5th percentile = -162 cells; 95th percentile = 119 cells) cells colonised eight years after EAB arrival in 2031 (Fig. 6). EAB arrival in 2031 therefore decreased the probability of EAB presence for 46% of cells with ash (increased for 31%; unchanged for 23%) and increased the number of cells with ash that recorded no EAB during any iteration to 10.7% (Online Resource 1, Figs. S56-S57).

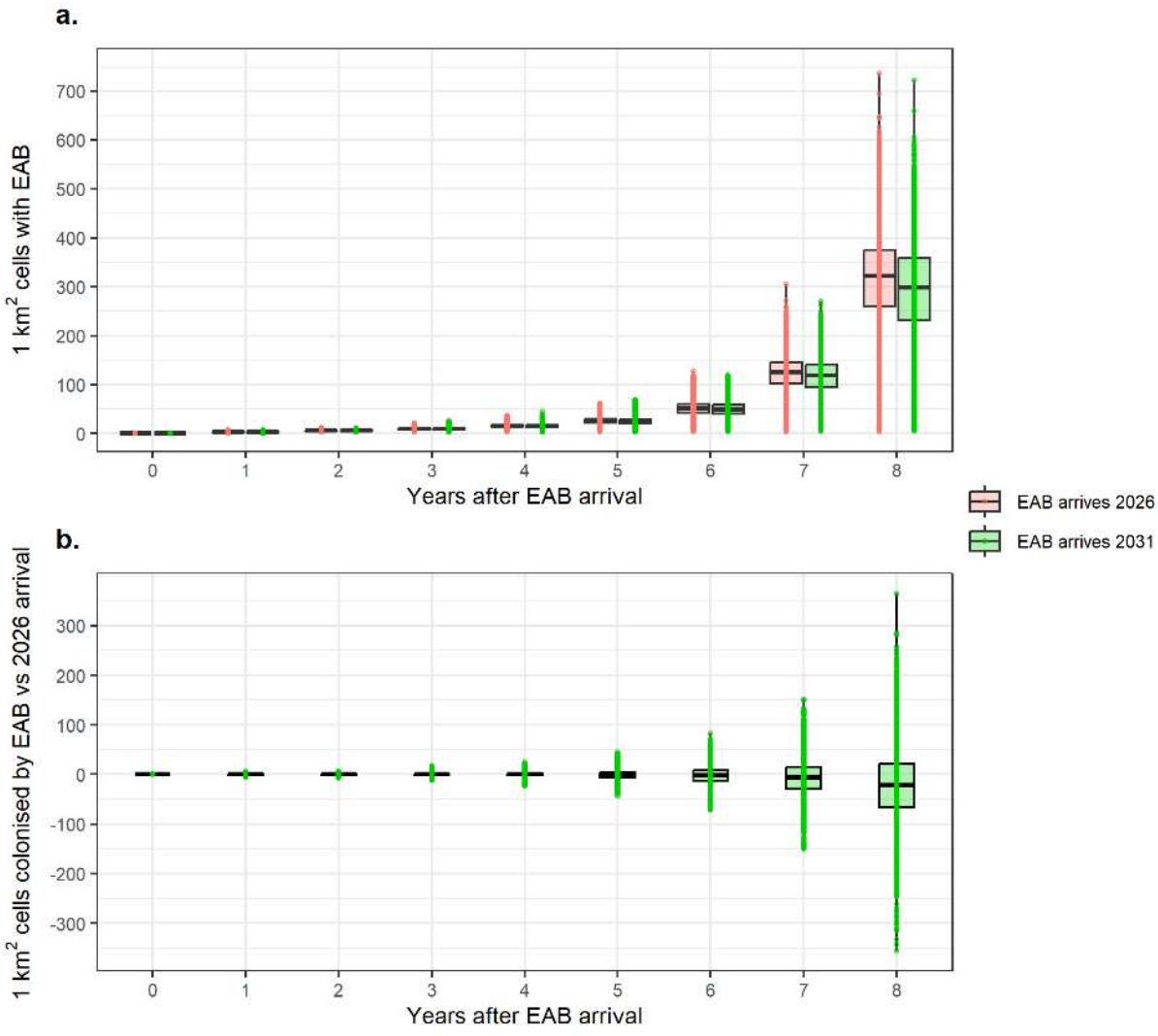


Fig. 6 Impact of EAB arrival year (2026 or 2031; Table 2) on EAB spread for each of the 9993 model iterations. (a) Boxplot of the number of 1 km^2 cells colonised by EAB for each scenario up to eight years after EAB arrival; (b) the number of 1 km^2 cells colonised by EAB following arrival in 2031 compared to 2026

Exploring the impact of different ADB progression rates

Changing the rate of ADB progression impacted the rate of EAB spread (Fig. 7). In comparison to the median ADB progression rate, the low ADB progression rate scenario increased EAB spread eight years after arrival by a median 30 cells (5^{th} percentile = -125 cells; 95^{th} percentile = 185 cells), whilst the high ADB progression rate scenario slowed EAB spread by a median of 36 cells (5^{th} percentile = -177 cells; 95^{th} percentile = 106 cells) (Fig. 7). Therefore, for the low ADB progression rate, 50% of cells with ash had an increased probability of colonisation (decreased for 29%; unchanged for 21%), whilst the number of cells with ash that recorded no EAB during any iteration decreased to 8.4% (Figs. S51-S52). Conversely, for the high ADB progression rate, 51% of cells with ash had a decreased probability of colonisation (increased for 26%; unchanged for 23%), whilst the number of cells with ash that recorded no EAB during any iteration increased to 11.2% (Figs. S53-S54).

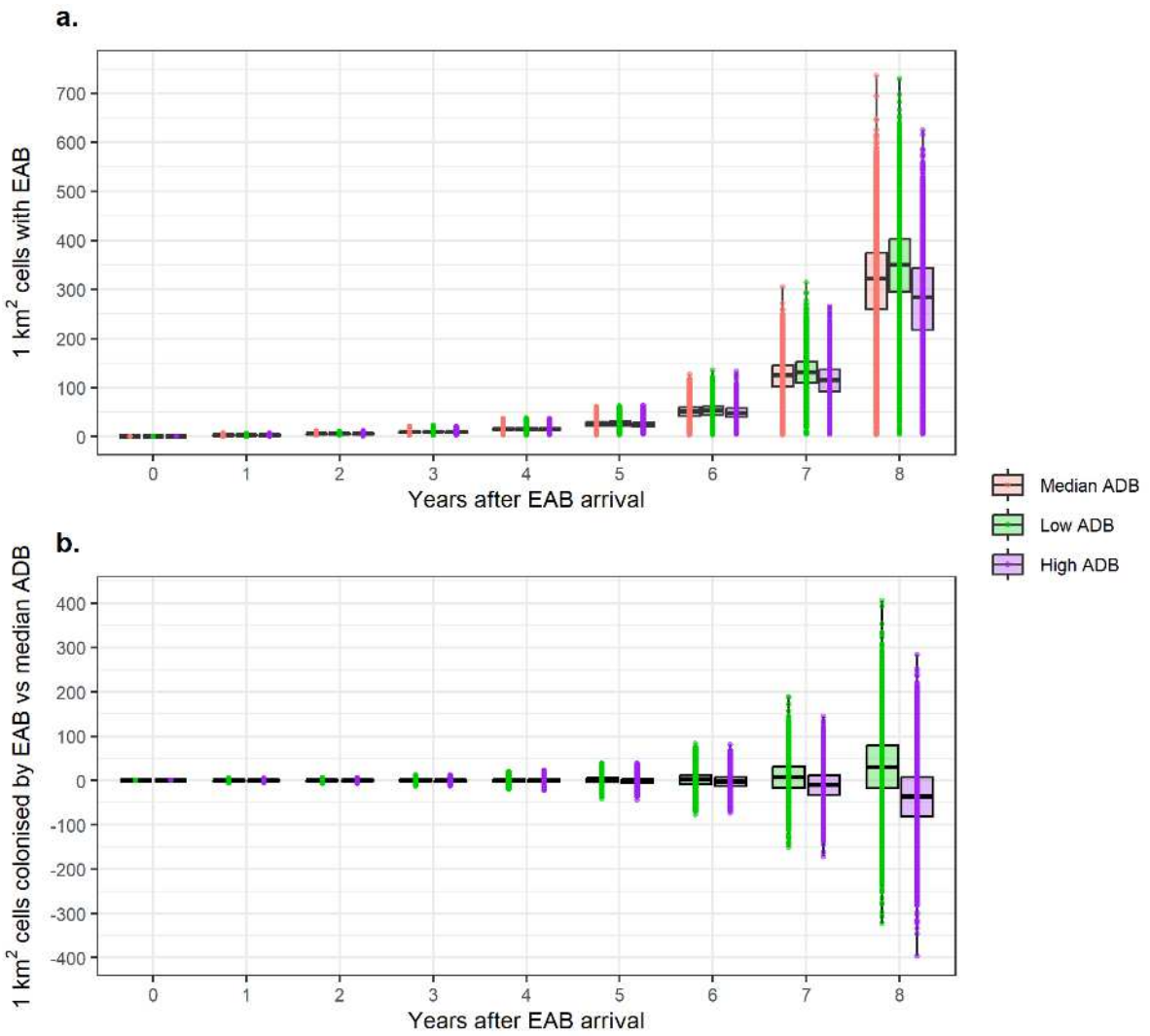


Fig. 7 Impact of ADB progress rate (Low, Median, High; Table 1; Table 2) on EAB spread for each of the 9993 model iterations. (a) Boxplot of the number of 1 km^2 cells colonised by EAB for each scenario up to eight years after EAB arrival; (b) the number of 1 km^2 cells colonised by EAB under the low and high ADB progress rate scenarios compared to the median ADB progress rate scenario

Discussion

This study provides the first spatial estimates of ADB impact in GB, as well as the first evidence for the landscape scale impacts of an endemic tree disease (ADB) on the invasion and spread of another exotic pest (EAB). Our model-based analysis revealed marked spatial variation in both tree mortality and stress across GB. These distributions of ADB severity across GB are predicted to similarly induce spatial variation in the population dynamics of EAB.

The baseline scenario (i.e. ADB progression at median estimates (Table 1), and the most likely impacts on EAB (Table 2)) resulted in a slower spread rate of EAB than when ADB was not included in the model (Fig. 4). The reduced spread of EAB in the presence of ADB was related to fewer ash hosts (Fig. 4) and our results show a strong positive relationship between the density of ash trees within EAB invaded cells, and the total spread of EAB, with the overall spread of EAB also being strongly positively related to the density of ash in the arrival location. Given that under the median ADB scenario, a median of 26.4% of ash trees were removed by 2026, with a minimum value of 9.3% and a maximum value of 60.2%, our results support a spatially variable impact of ADB host removal in the initial EAB arrival location and during following years on subsequent EAB spread. These findings concur with previous studies from North America which found that the spread of the beetle (Ward et al. 2020; Liebhold et al. 2025) is positively related to the host density. Furthermore, removing ash from areas already under EAB infestation in North

664 America slowed the spread of the beetle by a combination of removing available hosts and
665 killing EAB larvae (Fahrner et al. 2017).

666 A positive impact of high host density on pest spread may seem self-evident, but previous
667 research has produced contrary findings. For example, Ward et al. (2022) found that EAB
668 presence was not related to ash biomass or richness at the US county level. Mercader et al.
669 (2011b) also found that lower ash density can increase EAB spread rate through density-
670 dependent effects that enhance EAB development time. Our findings further the previous
671 research on relationships between host abundance and pest spread, by combining a population
672 dynamics model for EAB and a compartmental model for ADB to highlight the cascading impact
673 of an endemic disease to slow the invasion of another pest via removal of available hosts from
674 the landscape.

675 We found a small impact of EAB colonisation preference for ADB-stressed ash on the spread of
676 the beetle when larval survival rates were unchanged (Online Resource 1, Fig. S41). Preferential
677 oviposition on a subset of trees can constrain beetle spread by increasing density-dependent
678 larval mortality. At local scales, where the distribution of ADB severity categories may be more
679 variable, EAB preferential oviposition could focus on an even smaller subset of trees and
680 potentially constrain beetle spread even more. Early surveys indicate a positive association
681 between ADB- and EAB-affected trees (Davydenko et al. 2022), but more quantitative, finer
682 resolution data on EAB preferences across ADB stress levels is essential to reliably estimate
683 EAB spread.

684 Impacts of ADB on EAB were heavily dependent on the mortality rate of EAB larvae on ADB
685 stressed or recently dead trees (Fig. 5). Parameterising the EAB population dynamics model
686 based on experimental data for host drought stress, we highlight that under the upper elevated
687 larval mortality scenario (EAB mortality rate on S trees 1.66 times greater than E, 2.33 times
688 greater than I, 3 times greater than D) ADB greatly increases the spread of the beetle. The lower

elevated larval mortality scenario (EAB mortality rate on S trees 1.17 times greater than E, 1.33 times greater than I, 1.5 times greater than D) increased EAB spread relative to the baseline ADB model, but critically, the spread of EAB was similar to the model runs excluding the impacts of ADB.

Impacts of ADB on EAB larval mortality are still uncertain. Recent research from *H. fraxineus* stem wound inoculations found no impact of ADB infection on EAB larval development (Eisenring et al. 2026), but this is likely to differ under field scenarios where infection occurs through repeated exposure of foliage to *H. fraxineus* ascospores. It is also possible that both constitutive and induced (i.e. in response to ADB infection) defence responses can provide cross-resistance to EAB (Johnson and Whitehill 2023). Nevertheless, despite uncertainties regarding ADB impacts on EAB larval mortality, our results highlight that quantifying these parameters are critical for understanding EAB spread at the landscape scale.

There is an absence of ash condition monitoring across Europe to provide data on the ongoing impacts of ADB at a fine resolution at the landscape scale. We therefore parameterised an ADB compartmental model based on data from the European literature, and then examined the impacts of different rates of ADB progression on EAB spread. We found that EAB spread was sensitive to differences in ADB progress with higher rates of ADB progress resulting in slower EAB spread (Fig. 7). Moreover, progressing ADB for longer by delaying EAB arrival reduced beetle spread (Fig. 6). Our results emphasise the necessity of understanding the current impacts of ADB at the landscape scale. Large-scale ash tree condition surveys should become much more practical in future through use of remote sensing (Combes et al. 2024), which would enable clearer understanding of the spatial and temporal transition of individual trees through canopy decline and associated environmental influences.

There are large uncertainties on future ADB progress. The causal agent of the disease, *H. fraxineus*, has limited growth ability at 30°C (Kowalski and Bartnik 2010) and modelling from

France supports a negative relationship on ADB with the maximum daily temperature above 28°C (Fritsch et al. 2026). Previously, these temperatures were not typical in GB, but an increasing frequency of summer heatwaves could limit the severity of ADB, particularly in southern regions of GB. Additionally, although only a small proportion of trees appear resistant to ADB (McKinney et al. 2014), resistance to the disease is a polygenic trait and there is recent evidence for natural selection in regenerating ash (Metheringham et al. 2025). Whether there is sufficient standing resistance within woodlands, and whether the rate of genetic shift is occurring fast enough is still uncertain (Metheringham et al. 2025). However, given that tree vigour is strongly associated with ADB severity (Klesse et al. 2021), additional stress on trees from EAB could also enhance ADB impact. In this study, due to a lack of reliable data, we limited model complexity and used a static ash population with the primary goal of the research to understand potential impacts of ADB on EAB spread.

In summary, this study provides estimates of the impacts of ADB in GB based on its estimated arrival time, regional environmental conditions and disease dynamics, highlighting ADB's spatial variability within the landscape, and a basis to expand on this approach through additional scenarios (e.g. different distributions of ADB severity and transition parameters) and with further data and to inform policies aimed at the survival of ash in the face of ADB. By adapting a population dynamics model of EAB in GB (Alonso Chávez et al. 2025) to include the modelled distributions of ADB impact in GB, we demonstrate that EAB spread is most likely slowed by ADB. This is mainly dependent on ADB-related host removal, with ADB impacts on EAB spread thus depending on both the initial ash density and ADB severity in the arrival location and wider landscape. Elevated density-dependent larval mortality due to preferential attraction to ADB stressed trees also slows beetle spread, but to a lesser extent. Critically, a lower larval mortality on ADB stressed trees can potentially result in ADB greatly increasing EAB spread. Further field or experimental evidence on the relative attraction and survival rates of EAB on ADB affected hosts would help refine predictions based on this trade off. We also

highlight that on average, ADB impact on the pest does not begin to become apparent until at least six years after arrival under any examined scenario, but understanding ADB in the landscape, and the impact of ADB on EAB and ADB will be critical for determining most effective delimitation strategies and the feasibility of control measures.

Our results show that interactions between existing and emerging tree pests and diseases are not simply an ecological complexity but a key determinant of invasion dynamics. Failure to account for the impacts of ADB on EAB would produce incomplete, and potentially inaccurate, predictions of EAB spread and population dynamics. Consequently, predictive models and risk assessments should explicitly incorporate such interactions where possible. Beyond the EAB–ADB system, our findings underscore the need for continued monitoring of current pest and disease impacts, as these may strongly influence the trajectory of future biological invasions. Integrating these interactions into surveillance, modelling and policy frameworks will improve preparedness and support more effective management of emerging tree health threats.

References

Alonso Chávez V, Brown N, Parnell S, et al (2026) Surveillance of ash trees under multiple threats: Integrating emerald ash borer and ash dieback dynamics with stakeholder behaviour. J Appl Ecol 63:e70304. https://doi.org/10.1111/1365-2664.70304

Alonso Chávez V, Brown N, van den Bosch F, et al (2025) Early detection strategies for invading tree pests: Targeted surveillance and stakeholder perspectives. J Appl Ecol 62:857–871. https://doi.org/10.1111/1365-2664.70009

Bebber DP, Maclean IMD, Mosedale JR, Youngman BD (2025) Potential impacts of plant pests and diseases on trees and forests in the United Kingdom. Plants People Planet 7:1538–1550. https://doi.org/10.1002/ppp3.70023

Børja I, Timmermann V, Hietala AM, et al (2017) Ash dieback in Norway – current situation. In: Vasaitis R, Enderle R (eds) Dieback of European Ash (*Fraxinus* spp.) – Consequences and Guidelines for Sustainable Management. Swedish University of Agricultural Sciences, Uppsala, Sweden, pp 166–175

Brown N, Alonso Chávez V, Milne AE, Parnell S (2023) Host map of Ash trees in Great Britain. https://doi.org/10.23637/rothamsted.98y37

Byrd RH, Lu P, Nocedal J, Zhu C (1995) A limited memory algorithm for bound constrained optimization. SIAM J Sci Comput 16:1190–1208. https://doi.org/10.1137/0916069

Cleary M, Nguyen D, Marčiulynienė D, et al (2016) Friend or foe? Biological and ecological traits of the European ash dieback pathogen *Hymenoscyphus fraxineus* in its native environment. Sci Rep 6:21895. https://doi.org/10.1038/srep21895

Cobb RC, Haas SE, Kruskamp N, et al (2020) The magnitude of regional-scale tree mortality caused by the invasive pathogen *Phytophthora ramorum*. Earth's Future 8:e2020EF001500. https://doi.org/10.1029/2020EF001500

Combes M, Webber J, Boddy L (2024) Current understanding and future prospects for ash dieback disease with a focus on Britain. Forestry 97:678–691. https://doi.org/10.1093/forestry/cpae040

Davydenko K, Skrylnyk Y, Borysenko O, et al (2022) Invasion of emerald ash borer *Agrilus planipennis* and ash dieback pathogen *Hymenoscyphus fraxineus* in Ukraine—A Concerted Action. Forests 13:789. https://doi.org/10.3390/f13050789

Desprez-Loustau M-L, Balci Y, Cornara D, et al (2021) Is *Xylella fastidiosa* a serious threat to European forests? Forestry 94:1–17. https://doi.org/10.1093/forestry/cpaa029

Drogvalenko AN, Orlova-Bienkowskaja MJ, Bieńkowski AO (2019) Record of the emerald ash borer (*Agrilus planipennis*) in Ukraine is confirmed. Insects 10:338. https://doi.org/10.3390/insects10100338

Eisenring M, Roe A, Queloz V, et al (2026) A recent ash dieback infection neither affects emerald ash borer performance nor triggers a substantial systemic phytochemical defense response in European ash. J Pest Sci 99:44. https://doi.org/10.1007/s10340-025-01981-4

EPPO (2007) First report of *Agrilus planipennis* in the region of Moscow, Russia. EPPO Reporting Service no. 04-2007, article 2007/067. https://gd.eppo.int/reporting/article-1038. Accessed 27/10/2026.

EPPO (2025) First report of *Agrilus planipennis* in Belarus. EPPO Reporting Service no. 09-2025, article 2025/208. https://gd.eppo.int/reporting/article-8223. Accessed 27/10/2026.

EPPO (2026a) First report of *Agrilus planipennis* in Hungary. EPPO Reporting Service no. 06-2026, article 2026/137. https://gd.eppo.int/reporting/article-8433. Accessed 27/10/2026.

EPPO (2026b) First report of *Agrilus planipennis* in Slovakia. EPPO Reporting Service no. 07-2026, article 2026/163. https://gd.eppo.int/reporting/article-8459. Accessed 27/10/2026.

Fahrner SJ, Abrahamson M, Venette RC, Aukema BH (2017) Strategic removal of host trees in isolated, satellite infestations of emerald ash borer can reduce population growth. Urban For Urban Green 24:184–194. https://doi.org/10.1016/j.ufug.2017.03.017

FAO, IIASA (2023) Harmonized World Soil Database Version 2.0. Rome and Laxenburg. https://doi.org/10.4060/cc3823en

Forestry Commission (2013) National Forest Inventory estimates of quantities of broadleaved species in British woodlands, with special focus on ash. Forestry Commission, Edinburgh.

Fritsch C, Grosdidier M, Gégout-Petit A, Marçais B (2026) Mechanistic-statistical model for the expansion of ash dieback. Theor Popul Biol 171:1–21. https://doi.org/10.1016/j.tpb.2026.06.006

Fuchs S, Häuser H, Peters S, et al (2024) Ash dieback assessments on intensive monitoring plots in Germany: influence of stand, site and time on disease progression. J Plant Dis Protect 131:1355–1372. https://doi.org/10.1007/s41348-024-00889-y

Galassi M, Davies J, Theiler J, et al (2009) GNU Scientific Library reference manual, 3rd edn. Network Theory Ltd, Bristol. ISBN 978-0954612078. http://www.gnu.org/software/gsl/

George J-P, Sanders TGM, Timmermann V, et al (2022) European-wide forest monitoring substantiate the neccessity for a joint conservation strategy to rescue European ash species (*Fraxinus* spp.). Sci Rep 12:4764. https://doi.org/10.1038/s41598-022-08825-6

Gossner MM, Perret-Gentil A, Britt E, et al (2023) A glimmer of hope – ash genotypes with increased resistance to ash dieback pathogen show cross-resistance to emerald ash borer. New Phytol 240:1219–1232. https://doi.org/10.1111/nph.19068

Grosdidier M, Scordia T, Ioos R, Marçais B (2020) Landscape epidemiology of ash dieback. J Ecol 108:1789–1799. https://doi.org/10.1111/1365-2745.13383

Herms DA, McCullough DG (2014) Emerald ash borer invasion of North America: History, biology, ecology, impacts, and management. Annu Rev Entomol 59:13–30. https://doi.org/10.1146/annurev-ento-011613-162051

Hlásny T, Modlinger R, Gohli J, et al (2025) Divergent trends in insect disturbance across Europe's temperate and boreal forests. Glob Change Biol 31:e70580. https://doi.org/10.1111/gcb.70580

IPPC Secretariat (2025) Glossary of phytosanitary terms. International Standard for Phytosanitary Measures No. 5. FAO on behalf of the Secretariat of the International Plant Protection Convention

Jennings D, Shrewsbury P (2015) Biotic mortality factors affecting emerald ash borer (*Agrilus planipennis*) are highly dependent on life stage and host tree crown condition. Bull Entomol Res 105:598–606. https://doi.org/10.1017/S0007485315000498

Johnson TD, Whitehill JGA (2023) A phoenix glimmers within the ashes: generalized defensive traits suggest hope for plants under attack by invasive pests. New Phytol 240:912–914. https://doi.org/10.1111/nph.19230

Jung T, Horta Jung M, Webber JF, et al (2021) The destructive tree pathogen *Phytophthora ramorum* originates from the Laurosilva forests of East Asia. J Fungi 7:226. https://doi.org/10.3390/jof7030226

Kartakis S, Jung T, Kriticos DJ, Wesseler J (2026) Modeling disease expression of *Phytophthora ramorum* to estimate potential economic impacts in European forests. For Ecol Manag 601:123367. https://doi.org/10.1016/j.foreco.2025.123367

Klesse S, Abegg M, Hopf SE, et al (2021) Spread and severity of ash dieback in Switzerland – Tree characteristics and landscape features explain varying mortality probability. Front For Glob Change 4:645920. https://doi.org/10.3389/ffgc.2021.645920

Kowalski T (2006) *Chalara fraxinea* sp. nov. associated with dieback of ash (*Fraxinus excelsior*) in Poland. For Pathol 36:264–270. https://doi.org/10.1111/j.1439-0329.2006.00453.x

Kowalski T, Bartnik C (2010) Morphological variation in colonies of *Chalara fraxinea* isolated from ash (*Fraxinus excelsior* L.) stems with symptoms of dieback and effects of temperature on colony growth and structure. Acta Agrobot 63:99–106. https://doi.org/10.5586/aa.2010.012

Laubray S, Buée M, Marçais B (2023) Evidence of a component Allee effect for an invasive pathogen: *Hymenoscyphus fraxineus*, the ash dieback agent. Biol Invasions 25:2567–2582. https://doi.org/10.1007/s10530-023-03057-9

Liebhold AM, Ethington M, Stadsvold B, Negron J (2025) Spread of the emerald ash borer, *Agrilus planipennis*, in the Front Range region of Colorado. Biol Invasions 27:42. https://doi.org/10.1007/s10530-024-03512-1

Lovett GM, Weiss M, Liebhold AM, et al (2016) Nonnative forest insects and pathogens in the United States: Impacts and policy options. Ecol Appl 26:1437–1455. https://doi.org/10.1890/15-1176

Macquarrie C, Crandall J, Danci A, et al (2025) Detection and delimitation of emerald ash borer on Canada's west coast. BioInvasions Rec 14:271–279. https://doi.org/10.3391/bir.2025.14.2.01

Marçais B, Husson C, Caël O, et al (2017) Estimation of ash mortality induced by *Hymenoscyphus fraxineus* in France and Belgium. Balt For 23:159–167.

McCullough DG (2019) Challenges, tactics and integrated management of emerald ash borer in North America. Forestry 93:197–211. https://doi.org/10.1093/forestry/cpz049

McKinney LV, Nielsen LR, Collinge DB, et al (2014) The ash dieback crisis: genetic variation in resistance can prove a long-term solution. Plant Pathol 63:485–499. https://doi.org/10.1111/ppa.12196

Mercader RJ, Siegert NW, Liebhold AM, McCullough DG (2011a) Simulating the effectiveness of three potential management options to slow the spread of emerald ash borer (*Agrilus planipennis*) populations in localized outlier sites. Can J For Res 41:254–264. https://doi.org/10.1139/X10-201

Mercader RJ, Siegert NW, Liebhold AM, McCullough DG (2011b) Influence of foraging behavior and host spatial distribution on the localized spread of the emerald ash borer, *Agrilus planipennis*. Popul Ecol 53:271–285. https://doi.org/10.1007/s10144-010-0233-6

Metheringham CL, Plumb WJ, Flynn WRM, et al (2025) Rapid polygenic adaptation in a wild population of ash trees under a novel fungal epidemic. Science 388:1422–1425. https://doi.org/10.1126/science.adp2990

Petrice T, Haack R (2007) Can emerald ash borer, *Agrilus planipennis* (Coleoptera: Buprestidae), emerge from logs two summers after infested trees are cut? Great Lakes Entomol 40:92–95. https://doi.org/10.22543/0090-0222.2178

Pušpure I, Matisons R, Laiviņš M, et al (2017) Natural regeneration of common ash in young stands in Latvia. Balt For 23:209–217.

R Core Team (2025) R: A language and environment for statistical computing. R Foundation for Statistical Computing, Vienna.

San-Miguel-Ayanz J, de Rigo D, Caudullo G, et al (2016) European Atlas of Forest Tree Species

Santini A, Ghelardini L, De Pace C, et al (2013) Biogeographical patterns and determinants of invasion by forest pathogens in Europe. New Phytol 197:238–250. https://doi.org/10.1111/j.1469-8137.2012.04364.x

Schertler E, Queloz V, Monteleone F, et al (2026) Resistance and tolerance mechanisms of common ash (*Fraxinus excelsior*) against the ash dieback pathogen *Hymenoscyphus fraxineus*: latest advances and knowledge gaps. Forestry 99:cpaf038. https://doi.org/10.1093/forestry/cpaf038

Schneider K, van der Werf W, Cendoya M, et al (2020) Impact of *Xylella fastidiosa* subspecies *pauca* in European olives. Proc Natl Acad Sci USA 117:9250–9259. https://doi.org/10.1073/pnas.1912206117

Showalter DN, Villari C, Herms DA, Bonello P (2018) Drought stress increased survival and development of emerald ash borer larvae on coevolved Manchurian ash and implicates phloem-based traits in resistance. Agric For Entomol 20:170–179. https://doi.org/10.1111/afe.12240

Sicard A, Saponari M, Vanhove M, et al (2021) Introduction and adaptation of an emerging pathogen to olive trees in Italy. Microb Genom 7:000735. https://doi.org/10.1099/mgen.0.000735

Timmermann V, Nagy N, Hietala A, et al (2017) Progression of ash dieback in Norway related to tree age, disease history and regional aspects. Balt For 23:150–158.

UK Met Office (2025) How much does it rain in the UK? https://weather.metoffice.gov.uk/learn-about/weather/types-of-weather/rain/how-much-does-it-rain-in-the-uk . Accessed 27/10/2026.

U.S. Department of Agriculture, APHIS (2025) Emerald Ash Borer (EAB) known infested counties. https://www.aphis.usda.gov/plant-pests-diseases/eab/eab-infestation-map. Accessed 27/10/2026.

Ward S, Fei S, Liebhold AM (2020) Temporal dynamics and drivers of landscape-level spread by emerald ash borer. J Appl Ecol 57:1020–1030. https://doi.org/10.1111/1365-2664.13613

Ward S, Liebhold A, Fei S (2022) Variable effects of forest diversity on invasions by non-native insects and pathogens. Biodivers Conserv 31:2575–2586. https://doi.org/10.1007/s10531-022-02443-4

Wei X, Reardon D, Wu Y, Sun J (2004) Emerald ash borer, *Agrilus planipennis* Fairmaire (Coleoptera: Buprestidae), in China: a review and distribution survey. Acta Entomol Sin 47:679–685

Wickham H (2016) ggplot2: Elegant Graphics for Data Analysis. Springer-Verlag, New York. https://ggplot2.tidyverse.org

Wouters H (2021) Downscaled bioclimatic indicators for selected regions from 1979 to 2018 derived from reanalysis. Copernicus Climate Change Service (C3S) Climate Data Store (CDS). https://doi.org/10.24381/cds.fe90a594

Statements and Declarations

Funding

The work was funded by the United Kingdom's Research and Innovation (UKRI) Programme through the Natural Environment Research Council (NERC) (https://www.ukri.org/councils/nerc/) (Project: NE/T007729/1).

Competing interests

The authors have no relevant financial or non-financial interests to disclose.

Author Contributions

Conceptualization: Matt Combes, Vasthi Alonso Chávez, Alice Milne, Nathan Brown, Stephen Parnell; Formal analysis: Matt Combes, Vasthi Alonso Chávez, Alice Milne, Stephen Parnell; Funding acquisition: Vasthi Alonso Chávez, Alice Milne, Nathan Brown, Stephen Parnell; Methodology: Matt Combes, Vasthi Alonso Chávez, Alice Milne, Nathan Brown, Stephen Parnell; Project administration: Alice Milne; Supervision: Stephen Parnell; Writing – original draft preparation: Matt Combes, Stephen Parnell; Writing – review and editing: Matt Combes, Vasthi Alonso Chávez, Alice Milne, Nathan Brown, Stephen Parnell.

Data availability statement

946 The code and data used for the manuscript are available

947 https://github.com/MCombess/ADB_impact_on_EAB_GB_Manuscript and archived

948 https://doi.org/10.5281/zenodo.23512457.

949

950 Supplementary information

951 Online Resource 1 contains supplementary figures S1-S57.

Supplementary Files

This is a list of supplementary files associated with this preprint. Click to download.

- ESM1.docx